New Tools for Classification and Evaluation of Filtering Errors in Color Image Denoising

Fabrizio Russo

***Abstract*—**Performance analysis of color image denoising filters requires accurate measurements of many different effects produced during noise removal. Metrics in the literature consider only a subset of the filtering features that should be taken into account to address this issue. The novel set of metrics described in this paper aims at providing the necessary tools for analyzing the quality of a filtered picture from the point of view of residual noise, detail blur and color distortion. The approach adopts the YC_bC_r color space and performs the decomposition of the mean squared error (MSE) into six different components. Each MSE component focuses on a different class of filtering errors affecting the luminance or chroma channels of the filtered image. In order to validate the approach, the exact values of the MSE components are theoretically evaluated for some important nonlinear filters and used for a comparison. Computer simulations dealing with color pictures corrupted by Gaussian and impulse noise show that the results are in very good agreement with the theoretical values and that the method can represent a useful resource for analyzing the behavior of a denoising algorithm.

***Keywords*—**Color images, image denoising, image filtering, image analysis.

I. Introduction

COLOR images are nowadays involved in a growing number of research and application areas. Since noise affects almost any image processing system, the development of noise reduction algorithms is of paramount importance. In this respect, the most challenging goal for any image denoising filter is to reduce noise while preserving the useful information embedded in the image data [1-6]. Therefore, quantitative evaluations of different filtering features such as residual noise, color distortion and detail blur are necessary in order to assess the objective quality of a filtering process. Recently, some different methods have been proposed for quality assessment of grayscale filtered images [7-9]. All of them have overcome the limitations of classical and perceptual quality metrics in evaluating the performance of a denoising filter. Indeed, it is known that classical scalar operators, such as the mean squared error (MSE) and the peak signal-to-noise ratio (PSNR), perform badly in distinguishing noise cancellation from detail preservation. The same problem also occurs for metrics that aims at mimicking human perception [10-14], because they are insensitive to different mixtures of residual noise and filtering distortion that yield the same loss of perceived image quality. Recently introduced vector metrics [15-16] have constituted an effective attempt to yield separate evaluations of key filtering features. In the vector approach the MSE is typically decomposed into two different components dealing with residual noise and collateral distortion, respectively. The decomposition algorithms have been progressively improved and the accuracy of the results has significantly increased. In comparison, few metrics are available for color image processing applications. They typically encompass scalar indexes such as the *normalized color difference* (NCD) [17], the *color PSNR* (CPSNR) [18], the *color quality index* (CQI) [19] and the *mean pixel distance* (MPD) [20]. Scalar metrics, however, cannot separate residual noise from collateral distortion, as previously observed for the case of grayscale pictures. On the other hand, the quality of a color image is very often evaluated by simply applying metrics for monochrome pictures to the luminance channel only. In all these cases, the chroma information is ignored. This paper describes a novel approach to objective quality evaluation of filtered images that aims at overcoming all the mentioned limitations. The new method operates in the YC_bC_r [21] color coordinate system. In this approach, the MSE is first decomposed into two main components dealing with the luminance (Y) and the chroma (C_bC_r) information respectively. Each main component is then decomposed into three subcomponents addressing different classes of filtering errors (residual noise only, collateral distortion only, mixed residual noise and collateral distortion). The method yields significant advantages over other metrics:

- it can analyze both the luminance and chroma information of a color picture;
- it can yield the true values of residual noise and filtering distortion, whereas all other metrics fail.

A new validation procedure is provided in the paper in order to evaluate the accuracy of the proposed approach. In this procedure well known examples of color filters are considered, such as the vector median (VM) and the vector sigma (VS) filters. For these nonlinear operators, the exact values of filtering errors caused by residual noise and collateral distortion are theoretically evaluated and used for a comparison. Furthermore, we show how the proposed metrics can easily measure the different behavior of scalar and vector operators for color image denoising.

The rest of the paper is organized as follows. Section II describes the novel method, Section III presents the procedure

F. Russo is with the Department of Engineering and Architecture, University of Trieste, Via A. Valerio 10, I-34127 Trieste, Italy (e-mail: rusfab@univ.trieste.it).

for metrics validation, Section IV discusses the results of many computer simulations and, finally, Section V reports the conclusions.

II. The Proposed Metrics

The RGB color coordinate system is very often adopted for image display, storage and processing [22]. Other color coordinate systems can be adopted too [23]. The YC_bC_r color space is a more appropriate choice if we want to separate luminance and chroma information. As is known [21], the YC_bC_r color coordinate system is commonly adopted for digital television and image compression. In the YC_bC_r model, the luminance is represented by the Y channel, whereas the C_b and C_r components deal with the chroma information. Formally, let $\mathbf{r}(i,j)=[r_1(i.j), r_2(i.j), r_3(i.j)]^T$, be the vector (in the YC_bC_r space) representing the pixel at spatial position (i,j) in the original noise-free image (i=1,…, N_1; j=1,…, N_2), where r_1, r_2 and r_3 briefly denote the Y, C_b and C_r components, respectively. Similarly, let $\mathbf{g}(i,j)=[g_1(i.j), g_2(i.j), g_2(i.j)]^T$ and $\mathbf{f}(i,j)=[f_1(i.j), f_2(i.j), f_3(i.j)]^T$ be the corresponding pixels in the noisy and in the filtered picture. Thus, the filtering error in the k-th channel (k=1,2,3) can be expressed by the following relationship:

$$e_k(i,j) = f_k(i,j) - r_k(i,j) \tag{1}$$

Now, we want to determine the residual noise and distortion components of the absolute error, namely $a_k(i,j)$ and $b_k(i,j)$, respectively:

$$\left| e_k(i,j) \right| = a_k(i,j) + b_k(i,j) \tag{2}$$

where $a_k(i,j) \geq 0,\ b_k(i,j) \geq 0$. In order to estimate these error components, the proposed method exploits additional information: the image that can be achieved by filtering the noise-free reference picture. Let $\mathbf{d}(i,j)=[d_1(i.j), d_2(i.j), d_3(i.j)]^T$ be the pixel at location (i,j) in the image that is obtained by applying to the reference pixel $\mathbf{r}(i,j)$ exactly the same processing that is applied to the noisy pixel $\mathbf{g}(i,j)$. In our approach, the $a_k(i,j)$ and $b_k(i,j)$ components are evaluated by the following rules.

1) if $d_k(i,j) \leq r_k(i,j) < f_k(i,j)$ then $a_k(i,j)=e_k(i,j)$ and $b_k(i,j)=0$;

2) if $r_k(i,j) < f_k(i,j) \leq d_k(i,j)$ then $a_k(i,j)=0$ and $b_k(i,j)=e_k(i,j)$;

3) if $r_k(i,j) \leq d_k(i,j) \leq f_k(i,j)$ then $a_k(i,j)=f_k(i,j)-d_k(i,j)$ and $b_k(i,j)=d_k(i,j)-r_k(i,j)$;

4) if $f_k(i,j) < r_k(i,j) \leq d_k(i,j)$ then $a_k(i,j)=-e_k(i,j)$ and $b_k(i,j)=0$;

5) if $d_k(i,j) \leq f_k(i,j) < r_k(i,j)$ then $a_k(i,j)=0$ and $b_k(i,j)=-e_k(i,j)$;

6) if $f_k(i,j) \leq d_k(i,j) \leq r_k(i,j)$ then $a_k(i,j)=d_k(i,j)-f_k(i,j)$ and $b_k(i,j)=r_k(i,j)-d_k(i,j)$.

Condition $d_k(i,j) \leq r_k(i,j) < f_k(i,j)$ (first rule) means that filtering a noisy pixel yields a positive error whereas filtering the corresponding noise-free pixel would produce a negative error. Thus, the actual error $e_k(i,j)$ is very likely to represent residual noise only. Conversely, condition $r_k(i,j) < f_k(i,j) \leq d_k(i,j)$ (second rule) means that filtering a noisy pixel yields a smaller error than filtering the corresponding noise-free pixel. Thus, the actual error $e_{i,j}$ is very likely to represent collateral distortion only. Condition $r_k(i,j) \leq d_k(i,j) \leq f_k(i,j)$ (third rule) means that filtering a noisy pixel gives a larger error than filtering the corresponding noise-free pixel. Since both errors are positive, both residual noise and collateral distortion are very likely to occur. Similar consideration apply to the remaining rules

Now, let the overall MSE, evaluated in the YC_bC_r color space, be expressed as follows:

$$\mathrm{MSE} = \frac{1}{N_1 N_2} \sum_{i=1}^{N_1} \sum_{j=1}^{N_2} \sum_{k=1}^{3} e_k^2(i,j) \tag{3}$$

In the proposed approach, the MSE is first divided into two main components, namely *luminance MSE* (LMSE) and *chroma MSE* (CMSE):

$$\mathrm{LMSE} = \frac{1}{N_1 N_2} \sum_{i=1}^{N_1} \sum_{j=1}^{N_2} e_1^2(i,j) \tag{4}$$

$$\mathrm{CMSE} = \frac{1}{N_1 N_2} \sum_{i=1}^{N_1} \sum_{j=1}^{N_2} \sum_{k=2}^{3} e_k^2(i,j) \tag{5}$$

Then, LMSE and CMSE are decomposed as follows:

$$\mathrm{LMSE} = \mathrm{LMSE}_a + \mathrm{LMSE}_b + \mathrm{LMSE}_c \tag{6}$$

$$\mathrm{CMSE} = \mathrm{CMSE}_a + \mathrm{CMSE}_b + \mathrm{CMSE}_c \tag{7}$$

$$\mathrm{LMSE}_a = \frac{1}{N_1 N_2} \sum_{i=1}^{N_1} \sum_{j=1}^{N_2} a_1^2(i,j) \tag{8}$$

$$\mathrm{LMSE}_b = \frac{1}{N_1 N_2} \sum_{i=1}^{N_1} \sum_{j=1}^{N_2} b_1^2(i,j) \tag{9}$$

$$LMSE_c = \frac{2}{N_1 N_2} \sum_{i=1}^{N_1} \sum_{j=1}^{N_2} a_1(i,j)\ b_1(i,j) \tag{10}$$

$$CMSE_a = \frac{1}{N_1 N_2} \sum_{i=1}^{N_1} \sum_{j=1}^{N_2} \sum_{k=2}^{3} a_k^2(i,j) \tag{11}$$

$$CMSE_b = \frac{1}{N_1 N_2} \sum_{i=1}^{N_1} \sum_{j=1}^{N_2} \sum_{k=2}^{3} b_k^2(i,j) \tag{12}$$

$$CMSE_c = \frac{2}{N_1 N_2} \sum_{i=1}^{N_1} \sum_{j=1}^{N_2} \sum_{k=2}^{3} a_k(i,j)\ b_k(i,j) \tag{13}$$

Let us focus on the LMSE. According to (8-10), it is decomposed into three subcomponents dealing with residual noise ($LMSE_a$), collateral distortion ($LMSE_b$) and mixed residual noise and distortion ($LMSE_c$).

The evaluation of $LMSE_c$ is one of the novelties of the proposed approach. Indeed, this MSE component takes into account the filtered pixels where both distortion and residual noise occur in the luminance channel. Previous MSE decomposition schemes for grayscale images [7,15,16] did not consider this quantity and, for this reason, their accuracy was limited. Similarly, $CMSE_a$, $CMSE_b$ and $CMSE_c$ respectively address residual noise, collateral distortion and mixed residual noise and distortion affecting the chroma information.

III. Theoretical Evaluation of the True MSE Components

In order to validate the proposed method, we shall evaluate the *true values* of all the mentioned MSE components (namely $TLMSE_a$, $TLMSE_b$, $TLMSE_c$, $TCMSE_a$, $TCMSE_b$ and $TCMSE_c$) for some well known denoising techniques: the vector median (VM) [2], the vector sigma (VS) [3] and the scalar median (SM) filters.

A. Vector median filter

For this operator, the error components $a_k^{(VM)}(i,j)$ and $b_k^{(VM)}(i,j)$ can be theoretically evaluated as follows. Formally, let $\mathbf{x}(i,j)=[x_1(i.j),\ x_2(i.j),\ x_3(i.j)]^T$, be the vector (in the RGB space) representing the pixel at spatial position (i,j) in the noisy image (i=1,…, N_1; j=1,…, N_2), where x_1, x_2 and x_3 briefly denote the R, G and B components, respectively. Let us consider a $(2N+1)\times(2N+1)$ window centered on $\mathbf{x}(i,j)$. Let W be the set of vector pixels inside the window: $W=\{\mathbf{x}_1, \mathbf{x}_2,.., \mathbf{x}_M\}$, where $M=(2N+1)^2$. Let D_n be the aggregate distance of the pixel $\mathbf{x}_n$ to the set of vectors W:

$$D_n = \sum_{m=1}^{M} D(\mathbf{x}_n, \mathbf{x}_m) \tag{14}$$

where $D(\mathbf{x}_n, \mathbf{x}_m)$ denotes an appropriate distance (or similarity) measure.

Thus, the ordering $D_{(1)} \le D_{(2)} \le ... \le D_{(M)}$ implies the same ordering for the corresponding vector pixels:

$$\mathbf{x}_{(1)} \le \mathbf{x}_{(2)} \le ... \le \mathbf{x}_{(M)} \tag{15}$$

The VM is defined as the pixel $\mathbf{x}^{(VM)}$, inside the window, whose distance to all other pixels is minimum. Thus, according to the ordered sequence (15), the output $\mathbf{y}^{(VM)}$ of the VM filter is yielded by:

$$\begin{aligned} \mathbf{y}^{(VM)}(i,j) &= \mathbf{x}_{(1)} \\ &= \mathbf{x}(i-u, j-v) \end{aligned} \tag{16}$$

where $(i-u_1,j-v)$ are the coordinates of $\mathbf{x}_{(1)}$ into the window $(-N\le u\le N,\ -N\le v\le N)$. Now, after performing the conversion to the YC_bC_r color space, let $\mathbf{r}(i.j)$ and $\mathbf{g}(i.j)$ denote the vector pixels at location (i,j) in the reference and in the noisy picture, respectively. Let $\eta_k(i.j)$ be the noise amplitude affecting the k-th component of $\mathbf{g}(i.j)$:

$$g_k(i,j) = r_k(i,j) + \eta_k(i,j) \tag{17}$$

Thus, the filtering error in the k-th channel can be expressed by the following relationship:

$$\begin{aligned} e_k^{(VM)}(i,j) &= g_k(i-u, j-v) - r_k(i,j) \\ &= r_k(i-u, j-v) - r_k(i,j) + \eta_k(i-u, j-v) \end{aligned} \tag{18}$$

Let $\alpha_k^{(VM)}(i,j)$ and $\beta_k^{(VM)}(i,j)$ denote the (signed) error components dealing with residual noise and collateral distortion:

$$\alpha_k^{(VM)}(i,j) = \eta_k(i-u, j-v) \tag{19}$$

$$\beta_k^{(VM)}(i,j) = r_k(i-u, j-v) - r_k(i,j) \tag{20}$$

Depending on the signs and amounts of $\alpha_k^{(VM)}(i,j)$ and $\beta_k^{(VM)}(i,j)$, the following cases can be considered (for the sake of simplicity, the pixel coordinates are omitted).

Case 1: if $\alpha_k^{(VM)}$ and $\beta_k^{(VM)}$ have the same signs, then $a_k^{(VM)} = \left|\alpha_k^{(VM)}\right|$ and $b_k^{(VM)} = \left|\beta_k^{(VM)}\right|$.

Case 2: if $\alpha_k^{(VM)}$ and $\beta_k^{(VM)}$ have different signs and $\left|\alpha_k^{(VM)}\right| > \left|\beta_k^{(VM)}\right|$ then $a_k^{(VM)} = \left|e_k^{(VM)}\right|$, $b_k^{(VM)} = 0$.

(a) (b) (c)

(d) (e) (f)

Fig.1 – 24-bit color images: (a) "Parrots" (b) "Lighthouse", (c) "Motorbike", (d) "Girl", (e) "Rapids", (f) "Sailboat".

Case 3: if $\alpha_k^{(VM)}$ and $\beta_k^{(VM)}$ have different signs and $\left|\alpha_k^{(VM)}\right| \le \left|\beta_k^{(VM)}\right|$ then $a_k^{(VM)} = 0$, $b_k^{(VM)} = \left|e_k^{(VM)}\right|$.

Finally, the true values of the MSE components are computed by setting $a_k = a_k^{(VM)}$ and $b_k = b_k^{(VM)}$ in (8-13).

B. Vector sigma filter

The vector sigma filter exploits the same vector ordering expressed by (15). Again, let us consider a $(2N+1)\times(2N+1)$ window centered on $\mathbf{x}(i,j)$ and let W be the set of vector pixels inside the window: $W=\{\mathbf{x}_1, \mathbf{x}_2, .., \mathbf{x}_M\}$, where $M=(2N+1)^2$. The output $\mathbf{y}^{(VS)}$ of the vector sigma operator is defined by the following relationships [3]:

$$\mathbf{y}^{(VS)}(i,j) = \begin{cases} \mathbf{x}_{(1)} & \text{if } D_{(M+1)/2} \ge T \\ \mathbf{x}_{(M+1)/2} & \text{otherwise} \end{cases} \quad (21)$$

$$T = \frac{M-1+\lambda}{M-1} D_{(1)} \quad (22)$$

where $D_{(1)}$ is the aggregate distance computed by (14) and associated with the vector median, $\mathbf{x}_{(M+1)/2}$ is the center pixel, and λ is the tuning parameter that controls the smoothing.

Since $\mathbf{x}_{(M+1)/2}=\mathbf{x}(i,j)$ and $\mathbf{x}_{(1)}=\mathbf{x}(i-u,j-v)$ (according to (16)), we can rewrite expression (21) as follows:

$$\mathbf{y}^{(VS)}(i,j) = \begin{cases} \mathbf{x}(i-u, j-v) & \text{if } D \ge T \\ \mathbf{x}(i,j) & \text{otherwise} \end{cases} \quad (23)$$

where $D=D_{(M+1)/2}$. As in the previous case, let $\mathbf{r}(i.j)$ and $\mathbf{g}(i.j)$ denote the vector pixels at location (i,j) in the reference and in the noisy picture after performing the conversion to the YC_bC_r color space. Again, let $\eta_k(i.j)$ be the noise amplitude affecting the k-th component of $\mathbf{g}(i.j)$.

(a) (b) (c)

Fig.2 – (a) "Parrots" image corrupted by mixed Gaussian and impulse noise, (b) processed by the 3×3 VM filter, (c) processed by the 7×7 VM filter.

The filtering error in the k-th channel can be expressed as follows:

$$e_k^{(VS)}(i,j) = \alpha_k^{(VS)}(i,j) + \beta_k^{(VS)}(i,j) \tag{24}$$

where:

$$\alpha_k^{(VS)}(i,j) = \begin{cases} \eta_k(i-u, j-v) & \text{if } D \geq T \\ \eta_k(i,j) & \text{otherwise} \end{cases} \tag{25}$$

$$\beta_k^{(VS)}(i,j) = \begin{cases} r_k(i-u, j-v) - r_k(i,j) & \text{if } D \geq T \\ 0 & \text{otherwise} \end{cases} \tag{26}$$

Depending on the signs and amounts of $\alpha_k^{(VS)}(i,j)$ and $\beta_k^{(VS)}(i,j)$, the residual noise and distortion components of the filtering error, namely $a_k^{(VS)}(i,j)$ and $b_k^{(VS)}(i,j)$, can be obtained as in the previous filter.

C. *Scalar median filter*

In the past years, the simplest denoising approach often consisted in the application of scalar filters to each channel separately [2]. However, this choice typically destroys the correlation between color components producing an annoying amount of filtering errors. We shall show in the next section how the proposed metrics can yield a quantitative evaluation of these effects. Focusing on the scalar median filter, the error components $a_k^{(SM)}(i,j)$ and $b_k^{(SM)}(i,j)$ can be theoretically evaluated as follows. Let us consider a $(2N+1)\times(2N+1)$ window centered on $\mathbf{x}(i,j)$ and let W_k be the corresponding set of (monochrome) pixels in the k-th channel (k=1,2,3): $W_k=\{x_{1,k}, x_{2,k},...,x_{M,k}\}$, where $M=(2N+1)^2$. Inside each set, let the pixel values be ordered in ascending order of magnitude:

$$x_{(1),k} \leq x_{(2),k} \leq ... \leq x_{(M),k} \tag{27}$$

The median in the k-th set is thus given by the following relationship:

$$\begin{aligned} y_k^{(SM)}(i,j) &= x_{\left(\frac{M+1}{2}\right),k} \\ &= x(i-u_k, j-v_k) \end{aligned} \tag{28}$$

where $(i-u_k, j-v_k)$ are the corresponding coordinates into the window $(-N\leq u_k \leq N, -N\leq v_k \leq N)$. After performing the conversion to the YC_bC_r color space, the filtering error in the k-th channel can be expressed as follows:

$$e_k^{(VS)}(i,j) = \alpha_k^{(SM)}(i,j) + \beta_k^{(SM)}(i,j) \tag{29}$$

where:

$$\alpha_k^{(VS)}(i,j) = \eta_k(i-u_k, j-v_k) \tag{30}$$

$$\beta_k^{(VS)}(i,j) = r_k(i-u_k, j-v_k) - r_k(i,j) \tag{31}$$

Like the previous cases, we can obtain the components of the filtering error addressing residual noise ($a_k^{(VS)}(i,j)$) and distortion ($b_k^{(VS)}(i,j)$).

IV Results of Computer Simulations

In this section we report the results of many experiments dealing with images of the well-known Kodak test set [24].

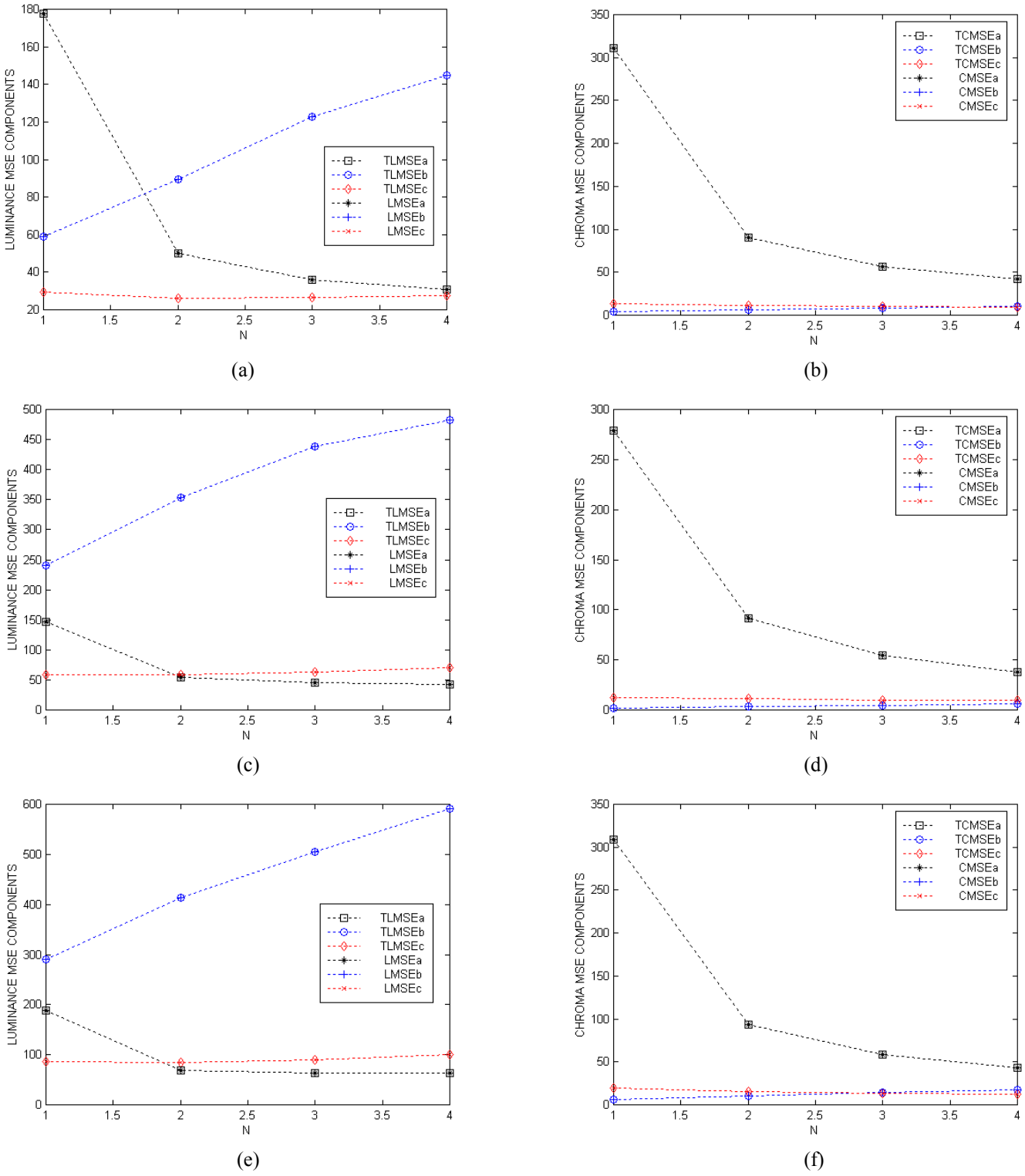

Fig.3 – Luminance and Chroma MSE components of images corrupted by Gaussian (σ=20) and impulse noise (p=0.4) and processed by (2N+1) × (2N+1) VM filters: "Parrots" (a)-(b), Lighthouse (c)-(d), "Motorbike" (e)-(f).

Six pictures from this set are considered: "Parrots", "Lighthouse", "Motorbike", "Girl", "Rapids" and "Sailboat". They are shown in Fig.1. All of these pictures are 24-bit color images whose size is 512-by-512 pixels. In the first group of experiments, we generated six noisy pictures by adding zero-mean Gaussian with standard deviation σ=20 and impulse noise with probability p=0.4. We processed the noisy data by adopting (2N+1) × (2N+1) VM filters with increasing window size in order to achieve different combinations of residual noise and filtering distortion.

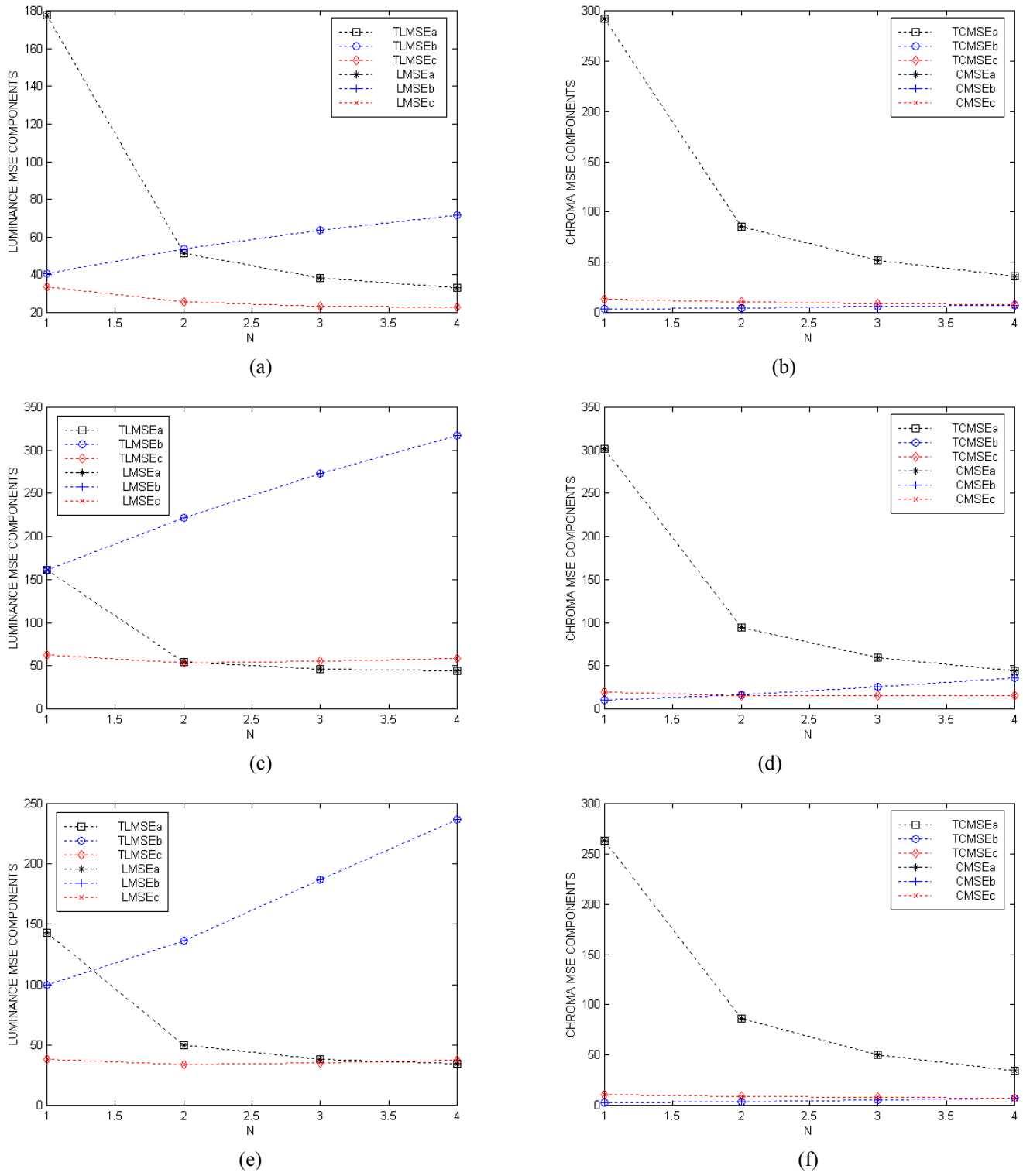

Fig.4 – Luminance and Chroma MSE components of images corrupted by Gaussian (σ=20) and impulse noise (p=0.4) and processed by (2N+1) × (2N+1) VM filters: "Girl" (a)-(b), "Rapids" (c)-(d), "Sailboat" (e)-(f).

For a comparison, we considered the theoretical results obtained in Section III. A sample of the data processed by the VM filter are shown in Fig.2 for visual inspection. The MSE components yielded by our method and the corresponding true values are graphically depicted in Fig.3 ("Parrots", "Lighthouse", "Motorbike") and Fig.4 ("Girl", Rapids", "Sailboat"). We can observe that, in all cases, the novel approach is in perfect agreement with the theoretical values. The behavior is correct. As the window size increases, the noise smoothing becomes stronger (lower values of $TLMSE_a$)

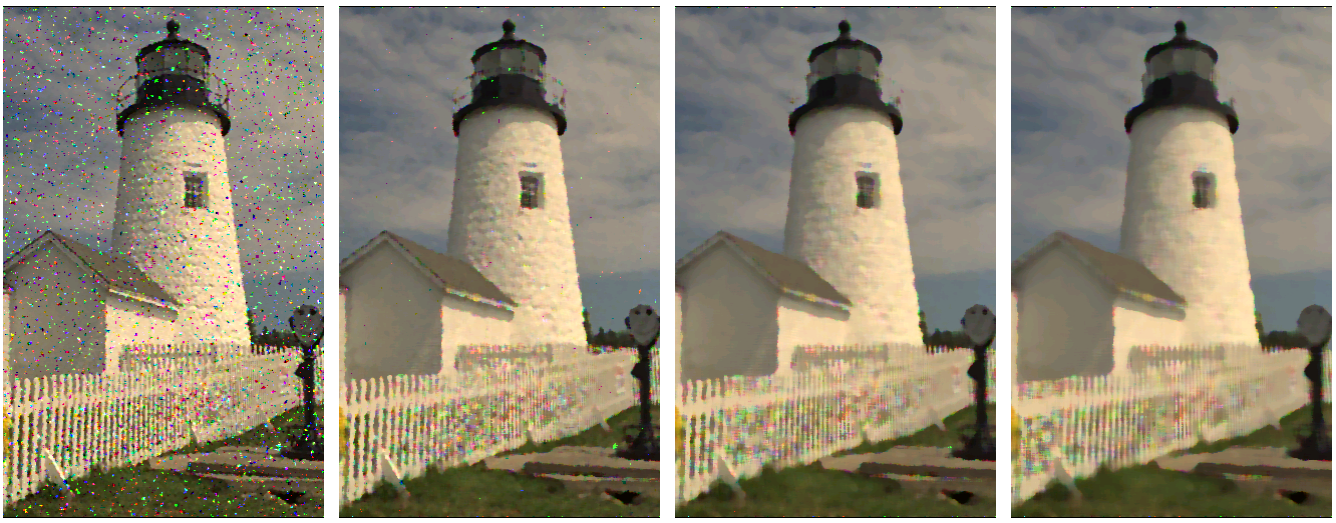

(a) (b) (c) (d)

Fig.5 – Portion of the "Lighthouse" image corrupted by impulse noise with probability 0.4 and processed by (2N+1)×(2N+1) scalar median filters: (a) N=1, (b) N=2, (c) N=3, (d) N=4.

(a) (b) (c) (d)

Fig.6 – Portion of the "Lighthouse" image corrupted by impulse noise with probability 0.4 and processed by (2N+1)×(2N+1) vector median filters: (a) N=1, (b) N=2, (c) N=3, (d) N=4.

and so becomes the filtering distortion (larger values of $TLMSE_b$), as it should be. The $TLMSE_c$ component is generally low and almost constant because it addresses pixels with mixed residual noise and collateral distortion. Indeed, as the window size becomes larger, the increase of collateral distortion is somewhat balanced by the corresponding decrease of residual noise. The behavior of the chroma components $TCMSE_a$ and $TCMSE_c$ is similar. Conversely, the $TCMSE_b$ (denoting chroma blur) is typically low because the denoising algorithm adopts a vector approach.

In the second group of experiments we considered the different effects of vector and scalar filtering. We corrupted the "Lighthouse" picture by superimposing impulse noise with probability p=0.4. Portions of this image processed by (2N+1)×(2N+1) scalar median filters are shown in Fig.5. Since the application of scalar medians disrupts the correlation among color components, a significant degradation of the chroma information is expected. This annoying effect is very apparent if we look at the originally white "fence" represented in the picture. The corresponding image data processed by (2N+1)×(2N+1) vector median filters are shown in Fig.6. The luminance distortion is similar (because it basically depends upon the window size), whereas the chroma errors are significantly lower, due to the vector approach.

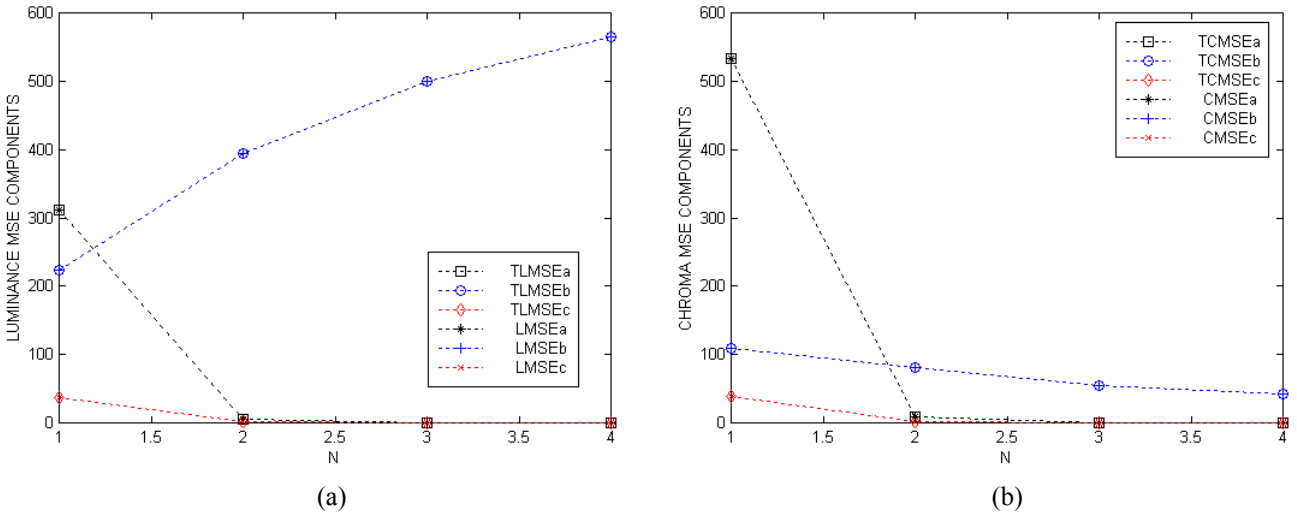

(a) (b)

Fig.7 – "Lighthouse" image corrupted by impulse noise with probability p=0.4 and processed by (2N+1×(2N+1) scalar median filters: (a) Luminace MSE components, (b) Chroma MSE components.

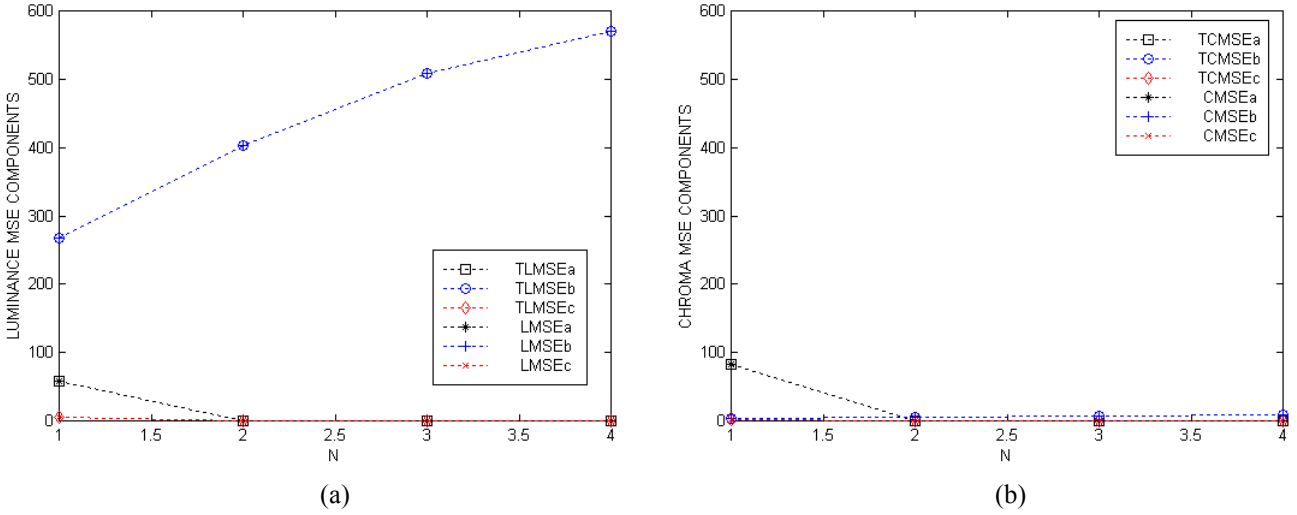

(a) (b)

Fig.8 – "Lighthouse" image corrupted by impulse noise with probability p=0.4 and processed by (2N+1×(2N+1) vector median filters: (a) Luminace MSE components, (b) Chroma MSE components.

The corresponding values of the MSE components are graphically reported in Fig.7 (scalar median) and Fig.8 (vector median). In order to highlight the different behavior of these filters, we adopted the same scale for all the graphs. If we focus on the luminance filtering errors (Figs.7a and 8a), we can see that the main effect (for N>1) is the distortion denoted by $LMSE_b$ and that this effect is about the same for scalar and vector filters having the same window size. For N>1, both $LMSE_a$ and $LMSE_a$ are negligible. On the contrary, if we focus on the chroma information (Figs.7b and 8b), we clearly see that the chroma distortion (measured by $CMSE_b$) is much higher for the scalar technique than for the vector method, as expected. (The $CMSE_A$ is also higher for N=1). In any case, the proposed MSE components are in perfect agreement with the theoretical values obtained in Section III.

In the third group of experiments we corrupted the test pictures by superimposing impulse noise with probability p=0.3 and we considered the application of the vector sigma filter. This is a very interesting method that preserves the details for large values of the tuning parameter λ., whereas it yields a growing cancellation of the noise as λ decreases. The MSE components given by our method and the corresponding true values are graphically depicted in Fig.9 ("Parrots", "Lighthouse", "Motorbike") and Fig.10 ("Girl", Rapids", "Sailboat").

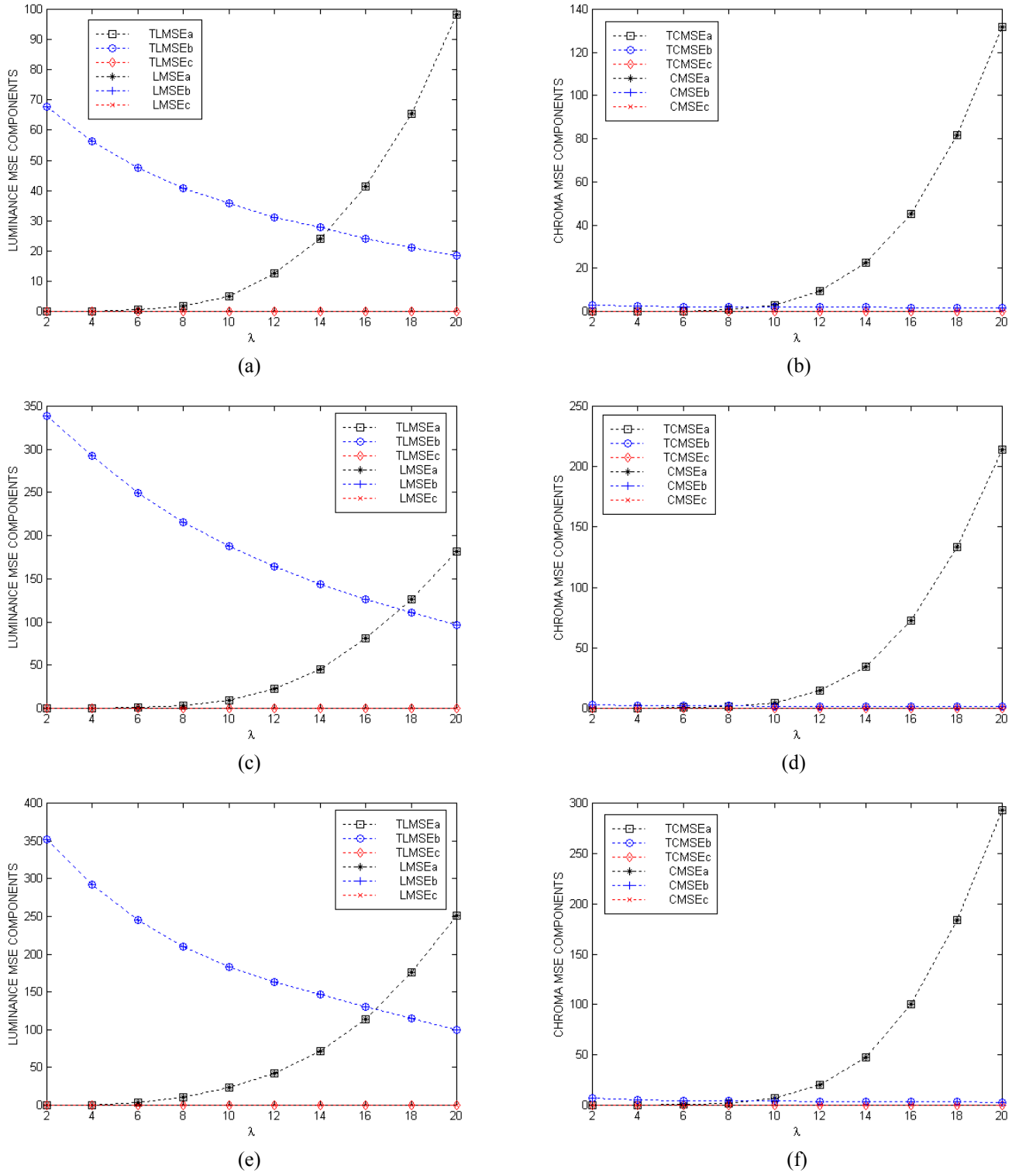

Fig.9 – Luminance and Chroma MSE components of images corrupted by impulse noise (p=0.3) and processed by a 5×5 vector sigma filter with different choices of the parameter λ: "Parrots" (a)-(b), Lighthouse (c)-(d), "Motorbike" (e)-(f).

If we consider the luminance information, we can see that the behavior of $LMSE_a$ and $LMSE_b$ is correct. As the filtering parameter λ increases, the value of $LMSE_a$ becomes larger, denoting more residual noise. Correspondingly, the value of $LMSE_b$ decreases because less distortion is produced. If we consider the chroma information, the $CMSE_a$ is the only relevant MSE component, whereas $CMSE_b$ and $CMSE_c$ are negligible. All the proposed MSE components perfectly estimates the theoretical values obtained in Section III. for this kind of denoising filter too.

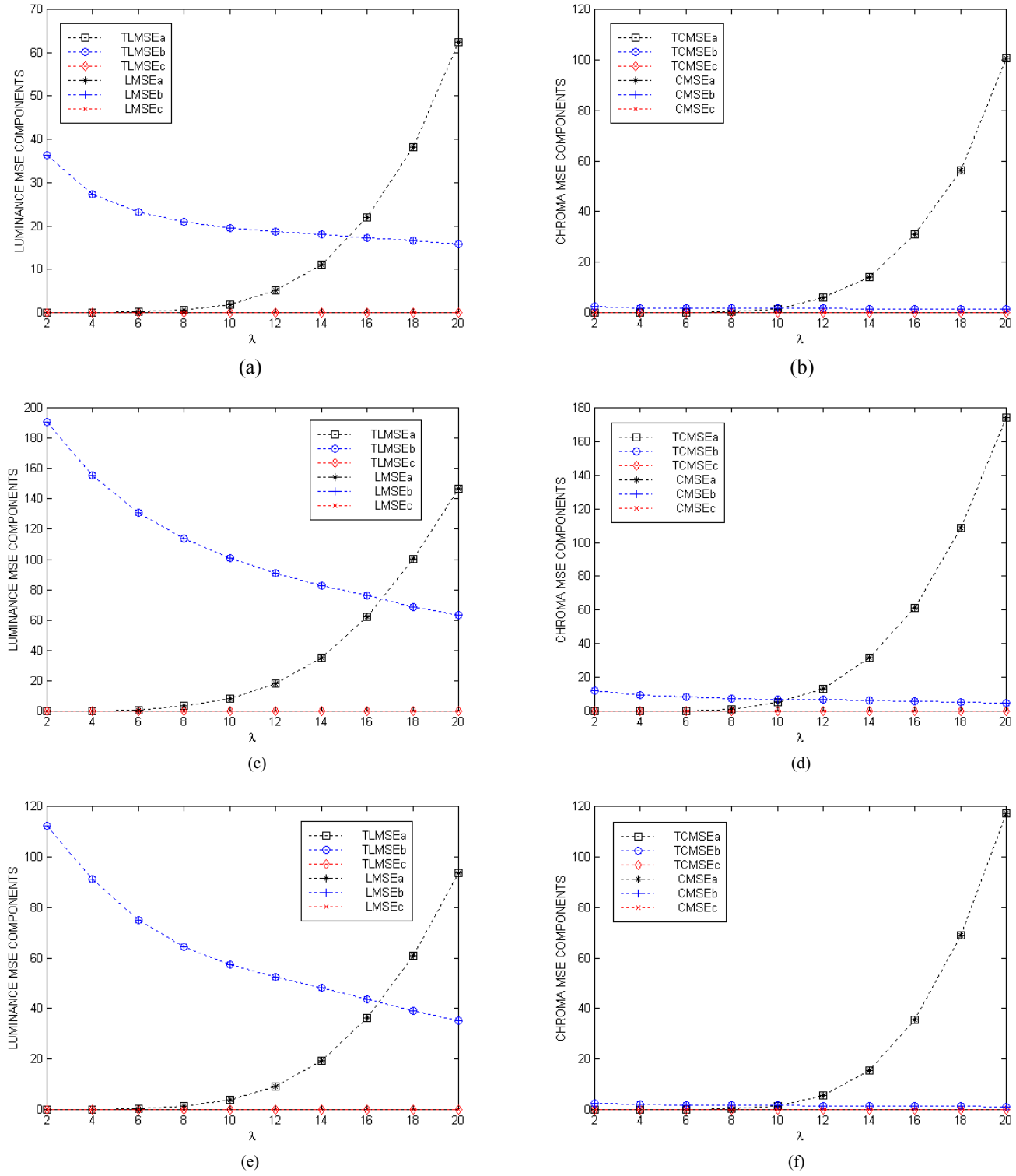

Fig.10 – Luminance and Chroma MSE components of images corrupted by impulse noise (p=0.3) and processed by a 5×5 vector sigma filter with different choices of the parameter λ: "Girl" (a)-(b), "Rapids" (c)-(d), "Sailboat" (e)-(f).

V. Conclusions

Quantitative evaluations of key filtering features such as residual noise, color distortion and detail blur are of paramount importance for analyzing the behavior of noise reduction filters for color images. The novel approach presented in this paper operates in the YCbCr color space in order to separate the luminance from the chroma filtering errors. The MSE is first decomposed into two main

components dealing with the luminance and chroma information, respectively. Thus, each main component is decomposed into three subcomponents addressing different distributions of filtering errors. With respect to previous techniques (e.g. vector metrics), the new method generates a larger number of MSE components for a deeper analysis of the filtering behavior. The accuracy of the proposed method has been investigated by adopting a new validation procedure. The true values of various MSE components have been theoretically evaluated for a collection of important nonlinear operators: the vector median, the vector sigma and the scalar median. Results of many computer simulations dealing with images corrupted by Gaussian and impulse noise have shown that the novel six-component approach is in very good agreement with such theoretical values. In particular, it can appraise the difference between scalar and vector filtering and give a quantitative evaluation of the various filtering effects.

REFERENCES

[1] F. Russo, "Objective Quality Assessment in Color Image Denoising: New Tools and Validation Procedures" Proc. NAUN 6th European Conference of Computer Science (ECCS '15), Rome, Italy, November 7-9, 2015, pp. 103-110.

[2] R. Lukac, B. Smolka, K. Martin, K. N. Plataniotis and A. N. Venetsanopoulos, "Vector filtering for color imaging", *IEEE Signal Processing Magazine*, 2005, pp.74-86.

[3] R. Lukac, B. Smolka, K. N. Plataniotis and A. N. Venetsanopoulos, "Vector Sigma Filters for Noise Detection and Removal in Color Images", *Journal of Visual Communication and Image Representation*, Vol.17, No.1, 2006, pp.1-26.

[4] S. Ling, Y. Ruomei, L. Xuelong and L. Yan, "From heuristic optimization to dictionary learning: a review and comprehensive comparison of image denoising algorithms", *IEEE Trans. on Cybernetics*, Vol.44, No.7, 2014, pp.1001-1013.

[5] A. Buades, B. Coll, and J. M. Morel, "A review of image denoising algorithms, with a new one", *Multiscale Model. Simul*.,Vol.4, No.2, 2005, pp.490-530.

[6] H. Bhujle, S. Chaudhuri, "Novel Speed-Up Strategies for Non-Local Means Denoising With Patch and Edge Patch Based Dictionaries", *IEEE Transactions on Image Processing*, Vol. 23, n.1, 2014, pp. 356–365.

[7] A. De Angelis, A. Moschitta, F. Russo and P. Carbone, "A Vector Approach for Image Quality Assessment and Some Metrological Considerations," *IEEE Transactions on Instrumentation and Measurement*, vol.58, n.1, 2009, pp. 14–25.

[8] F. Russo, "Performance Measurement of Image Filtering Systems Using the Peak Signal-to-Blur Ratio (PSBR)", Proc. NAUN 5th European Conference of Systems (ECS '14), Geneva, Switzerland, December 29-31, 2014, pp.19-26.

[9] F. Russo, " New Method for Measuring the Detail Preservation of Noise Removal Techniques in Digital Images", *WSEAS Transactions on Signal Processing,*, Vol. 11, Art. #38, 2015, pp. 317-327.

[10] Z. Wang, A. C. Bovik, H. R. Sheikh, and E. P. Simoncelli, "Image Quality Assessment: From Error Visibility to Structural Similarity", *IEEE Transactions on Image Processing,* vol.13, n.4, 2004, pp.600-612.

[11] D.-O. Kim and R.-H. Park, "New Image Quality Metric Using the Harris Response", *IEEE Signal Processing Letters,* vol.16, n.7, 2009, pp. 616–619.

[12] S. Winkler and P. Mohandas, "The Evolution of Video Quality Measurement: From PSNR to Hybrid Metrics", *IEEE Transactions on Broadcasting*, Vol.54, n.3, 2008, pp.660– 668.

[13] N. Ponomarenko, F. Battisti, K. Egiazarian, J. Astola, V. Lukin "Metrics performance comparison for color image database", Fourth international workshop on video processing and quality metrics for consumer electronics, Scottsdale, Arizona, USA. Jan. 14-16, 2009.

[14] A. Hore and D. Ziou, "Image Quality Metrics: PSNR vs. SSIM", Proc. 20th Int. Conf. on Pattern Recognition, 2010, pp.2366- 2369.

[15] F. Russo, "New Method for Performance Evaluation of Grayscale Image Denoising Filters", *IEEE Signal Processing Letters*, vol.17, n.5, 2010, pp.417-420.

[16] F. Russo, "New Vector Method for Quality Assessment in Image Denoising", Proc. NAUN 3rd Int. Conf. on Circuits, Communications, Computers and Applic., CSCCA'14, Florence, Italy, Nov. 22-24, 2014, pp.197-206.

[17] K. N. Plataniotis and A. N. Venetsanopoulos, Color Image Processing and Application. New York: Springer Verlag, 2000.

[18] N-X Lian, V. Zagorodnov and Y-P Tan, "Edge-Preserving Image Denoising via Optimal Color Space Projection", *IEEE Trans. on Image Processing,* vol.15, n.9, 2006, pp.2575-2587.

[19] A. Medda and V. DeBrunner, "Color Image Quality Index Based on the UIQI", 2006 IEEE Southwest Symposium on Image Analysis and Interpretation, pp. 213 – 217, 2006.

[20] M. E. Yuksel and A. Basturk, "Application of Type-2 Fuzzy Logic Filtering to Reduce Noise in Color Images", in *IEEE Computational Intelligence Magazine*, vol.7, no.3, August 2012, pp.25-35.

[21] W. Burger and M.J. Burge, "Digital image processing: an algorithmic introduction using Java", Springer, 2012.

[22] Szénási, S., "Distributed Region Growing Algorithm for Medical Image Segmentation", International Journal of Circuits, Systems and Signal Processing, 2014, Vol. 8, No.1, pp.173-181, ISSN 1998-4464.

[23] Sergyán, Sz., "Parameter Optimization of Dominant Color Histogram Descriptor in Content-Based Image Retrieval Systems", International Journal of Circuits, Systems and Signal Processing, 2014, Vol. 8, No.1, pp.286-291, ISSN 1998-4464.

[24] R. Franzen, "Kodak Lossless True Color Image Suite". http://r0k.us/graphics/kodak/

F. Russo is currently Associate Professor of electrical and electronic measurements in the Department of Engineering and Architecture of the University of Trieste, Italy. He is author/coauthor of more than 100 papers in international journals, textbooks, and conference proceedings including the Wiley Encyclopedia of Electrical and Electronics Engineering, (J. G. Webster ed.). His research interests presently include nonlinear and fuzzy techniques for image denoising, image enhancement and image quality measurement. He was one of the organizers of the 2004 and 2005 IEEE International Workshops on Imaging Systems and Techniques. He served as Technical Program Co-Chairman of the 2006 IEEE Instrumentation and Measurement Technology Conference and as Co-Guest Editor for the Special Issue of the IEEE Transactions on instrumentation published in August 2007. He was invited speaker of the plenary session "Fuzzy Models for Low-level Computer Vision: a Comprehensive Approach" at the IEEE Symposium on Intelligent Signal Processing (WISP 2007). He has served as session chairman/co-chairman in many conferences organized by IEEE, IMEKO, WSEAS and NAUN.